THIN FILM FLOWS NEAR ISOLATED HUMPS AND INTERIOR CORNERS

Gregory P. Chini,* Oliver E. Jensen** and John R. King**
* *Mechanical Engineering Department, University of New Hampshire, USA*
** *School of Mathematical Sciences, Nottingham University, Nottingham, UK*

INTRODUCTION

We examine the surface-tension-driven readjustment of a viscous liquid film following a sudden change in the shape of adjacent solid surfaces. Such situations arise widely in industrial contexts, e.g. when geometrical imperfections create defects in coatings. Important physiological applications arise in the lung, when the liquid lining of an airway redistributes following impact of an inhaled particle or contact between the wet walls of a collapsing airway. Here, an initially flat solid substrate is assumed to deform into an *isolated* hump or interior corner. For sufficiently tall humps and sharp corners, a quasi-static puddle connects to a spatially unbounded thin film; the capillary pressure in the film is greater than that in the puddle, causing it to grow. We employ numerical simulations and asymptotic analysis to characterise the induced flows. We then show that flows off humps with maxima less than a critical height have a qualitatively different structure.

MATHEMATICAL MODELS

We model the flow of a two-dimensional incompressible Newtonian fluid of constant viscosity μ bounded above by a passive gas and below by a rigid, possibly curved, stationary substrate. The surface tension σ acting at the free surface is assumed uniform and van der Waals forces are neglected. When gradients in substrate curvature vary over distances large compared to the fluid depth, the standard thin-film equation can be extended in an asymptotically consistent fashion (Schwartz & Weidner 1995), yielding

$$h_t \; + \; \tfrac{1}{3}\left[h^3(h+g)_{xxx}\right]_x \quad = \quad 0, \tag{1}$$

where the substrate and free-surface locations lie at $y = g(x)$ and $y = g(x)+h(x,t)$, respectively, in Cartesian (x, y)-coordinates, and t is time. We employ (1) to model capillary-driven flow off of a Gaussian-shaped hump, $g(x) = g_0 \exp[-(x/2d)^2]$, starting from the uniform initial condition $h(x, 0) = 1$. We examine solutions of (1) on a finite domain $0 \le x \le L$ but select $L \gg 1$ so that the film remains undisturbed near $x = L$. To model flows near an interior corner, where the substrate curvature is singular, we employ an alternative formulation: namely, Heil & White's (2002) modified thin-film equation,

$$\rho_t \; + \; \tfrac{1}{3}\left[h^3 k_s\right]_s \quad = \quad 0, \tag{2}$$

coupled to a parameterisation of the film thickness using spines. s measures distance along the flat substrate from the corner, while h measures the height of the film along certain prescribed directions (spines). The spine angle distribution, $\beta(s)$, is chosen so that the spines do not intersect within the fluid interior and are normal to the substrate where the film is thin. The film density $\rho(s,t) = h\cos\beta + \mathrm{d}\beta/\mathrm{d}s\, h^2/2$ then insures exact mass conservation. By employing the exact curvature of the free surface $k(s,t) = (y_{ss}x_s - x_{ss}y_s)/(x_s^2 + y_s^2)^{3/2}$, (2) enforces the exact Young–Laplace constraint in regions where the film is deep and quasi-steady. In regions where the film is thin, (2) reduces to the standard thin-film equation. Thus, the unsteady dynamics of thin-film regions and, hence, the fluid flux into (or out of) the corner puddle are accurately predicted.

RESULTS

In conjunction with symmetry and no-flux boundary conditions, (1) and (2) were discretised in space using 2nd-order accurate finite differences and advanced in time using an adaptive-step backward-differencing scheme. Most computations were carried out for $O(10^7)$ time units using $O(10^4)$ grid points. Large-hump simulations (e.g. $g_0 = 10$) were conducted with $L = 500$, while small-hump simulations (e.g. $g_0 = 2.8$) were conducted with $L = 5000$. For $d = 0.5$, a nonuniform grid was needed to provide adequate spatial resolution. An equispaced s-grid, however, was found to be adequate for corner simulations with $L = 30$, an initial puddle height (at $s = 0$) of 1.5, an initial far-field film thickness of 0.06 and an interior semi-angle of $\pi/5$. Raw numerical results for both the large-hump and corner simulations are shown in figure 1 [(a),(b)–free-surface locations; (c),(d)–pressure distributions]. Broadly similar behaviour is observed: following a transient phase (not depicted), the film pinches off, separating a quasi-static puddle from a propagating capillary

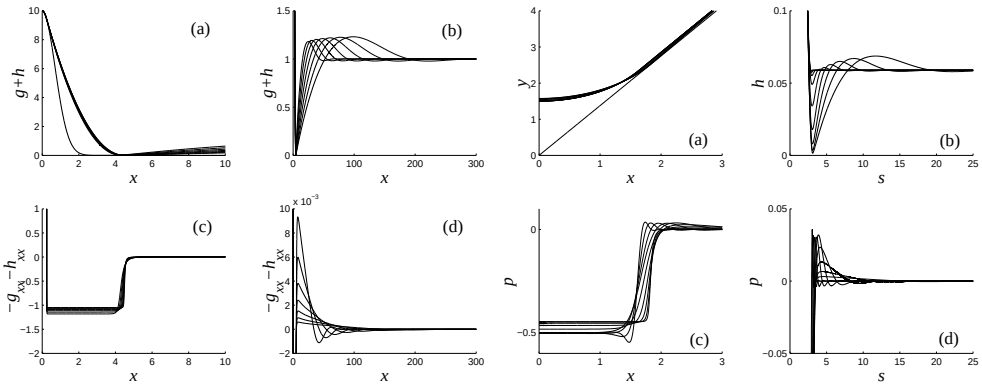

FIGURE 1. Raw simulation data for hump (left subplots) and corner (right subplots).

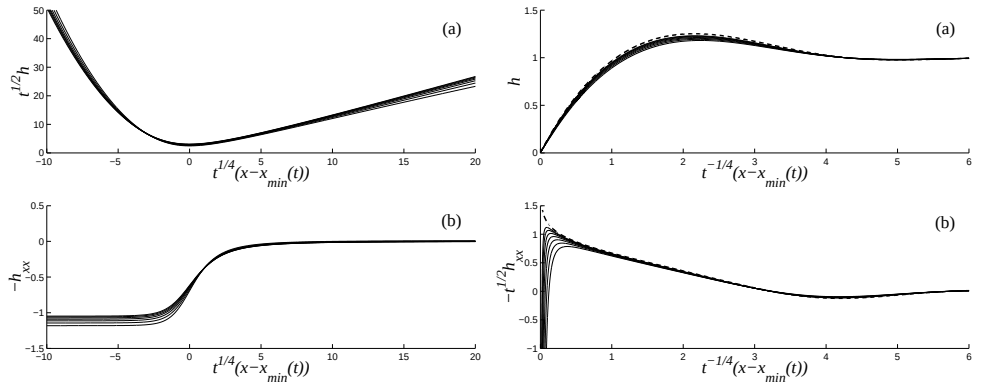

FIGURE 2. Scaled hump film height (upper) and pressure (lower) in regions II (left) and III (right).

wave. Large-time asymptotic analysis reveals that the slowly growing quasi-static puddle (region I) satisfies $h+g \sim \kappa(x-x_0^2)/2$, where κ and, hence, the volume V_I can be related to $g(x)$ and the effective contact line location $x_0(t)$ [$\approx x_{min}(t)$ in figure 2] via matching conditions. The right subplots in figure 2 indicate that the propagating wave (region III) can be captured by seeking a solution of the form $h(x,t) \sim F_0(\xi)+t^{-1/4}MF_1(\xi)$, where $x = x_0(t)+t^{1/4}\xi$ and M is a constant. The dashed lines show the leading-order solution $F_0(\xi)$, which satisfies $-\xi F_{0\xi}/4+(F_0^3F_{0\xi\xi\xi})_\xi/3=0$ (Bowen 1998, Aradian et al. 2001), and its negated second derivative. Since F_1 satisfies a linear equation, we have imposed the normalisation condition $\int_0^\infty F_1 \mathrm{d}\xi \equiv 1$. Region II is a quasi-steady draining region that acts as a valve – note the shock-like pressure distributions in figures 1c. In accord with the left subplots in figure 2 (and following Jones & Wilson 1978), we set $h \sim t^{-1/2}H(\eta)$, $x = x_0(t)+t^{-1/4}\eta$ and obtain $H^3H_{\eta\eta\eta} = -Q$ for some constant flux $Q>0$. Matching H with region I and H_η with region III determines Q in terms of $\kappa(x_0)$. Since $h(x,0)=1$ for $0<x<L$, the total fluid volume $V=L$ for all time. For large t, $V \sim V_I+V_{III}$. Using the equation governing F_0, the leading-order contribution to V_{III} is found to be $L-x_0$. Notably, an $O(1)$ fixed-mass contribution M arises from the F_1 correction, which, although $O(t^{-1/4})$, is spread over an $O(t^{1/4})$ distance. Thus, the volume condition becomes: $x_0 \sim V_I(x_0)+M$, where M – the mass of fluid trapped in (or lost from) region III – is determined by the transient dynamics over intermediate time scales. Following pinch-off, the puddle in region I grows very slowly: x_0 advances according to $V_I'(x_0)x_{0t} \sim Qt^{-5/4}/3$, i.e. $x_{0t} = O(t^{-5/4})$. Finally, simulations for small humps reveal a qualitatively different structure, with a propagating capillary wave attaching *directly* to the top of the hump. To describe this case, we expand $h(x,t)$ as in region III except that $x = t^{1/4}\xi$. We find two solution branches for $1<g_0<g_c$ and no solutions for $g>g_c$, where the critical hump height $g_c \approx 3.36$. Our small-hump numerical simulations converge to the branch of similarity solutions having smaller (negative) slope at the origin. For a given g_0, $M(g_0) = -\int_0^\infty (F_0-1)\mathrm{d}\xi$; i.e. since pinch-off does *not* occur for these small-hump solutions, $M(g_0)$ can be predicted.